

Original Article

Hardness Prediction of Wind Turbine Components Considering the Tempering Effect

Jong Soo Park¹, Seung Woo Kim¹, Hyoung Woo Lee², Ki Bong Han², Jin Mo Lee³, Jong Hun Kang^{#2}

¹Graduate School of Mechanical Engineering, Jungwon Univ.

²Aero-Mechanical Engineering, Jungwon Univ.

³R&D Center, Taewoong Co. Ltd.

#jhkang@jwu.ac.kr

Abstract - This study investigated the internal hardness and strength prediction of the main shaft component of large-scale wind turbines according to the heat treatment condition. In order to consider the mass effect from the cooling of large-scale components, cooling specimens were fabricated to carry out the hardenability test and tempering at 600°C and 660°C. The specimen hardness after quenching and tempering was measured by investigating the hardness distribution according to the distance from the Quench end. The quenched hardness variation of the large-scale cooling specimen was predicted for various locations using Deform and Jmatpro and compared with experiment results. For the hardness after tempering, the softening phenomenon from the experiment was formulated using the tempering parameter. The hardness was analyzed through fractured specimens for various locations of the main shaft manufactured by open die forging to determine the validity of the calculation formula. Comparison of the hardness and formula results revealed that reliable hardness prediction is possible using the proposed formula.

Keywords — Tempering Parameter, Holloman Jaffe Parameter, Jominy test, Mass effect, Hardness, Tensile strength

I. INTRODUCTION

The mechanical components of wind turbines are conventionally manufactured using open die forging. Large-scale forged products used in wind turbines include the main shaft, bearings, and tower flange, which transfers rotation power or provides support for structures.[1]~[3] The hardness and strength of large-scale forged parts for wind turbines vary for different points of the parts due to the differences in cooling rate during heat treatment. For the changes in hardenability and mechanical properties, taking into consideration the mass effect, research was carried out for standard specimens of 25mm length or specimens with thicknesses up to 100mm.[4]~[6] However, diameters of $\Phi 400\sim 1000\text{mm}$ are common for 2~5MW main shafts that are widely commercialized, and the cross-section thickness of slewing bearings increased up to 250~500mm so that

prediction of mechanical properties for the core part is difficult from the hardenability result of the standard specimen.

In this study, 42CrMo4 was fabricated into specimens with dimensions of 400x400x400mm, where the surface of one end was cooled to measure the hardness and microstructure of various points of the cooling specimen.[7],[8] For the quenching process, Deform and Jmatpro were used to calculate the hardness, strength, and volume fraction of phases for various points according to the cooling rate and compared with experimental results to evaluate the potential of a prediction model.[9]~[14] Since structural steel is used after quenching and tempering treatment, the hardness variation according to the tempering temperature was investigated. The hardness variation obtained through experimentation was formulated using the tempering parameter.[15]~[17]

In order to determine the coherence of the mechanical properties of large-scale forged parts, specimens were prepared from wind turbine components, and the tensile strength and hardness were measured. The hardness for various points of the main shaft according to the cooling condition and heat treatment was predicted considering the tempering conditions and compared with the experiment results of the specimens prepared from wind turbine parts to verify the validity of the hardness prediction method.

II. Quantitative Model fo the Mass Effect

A. Hardenability Test of Large Scale Specimens

The Jominy test method is a representative test method used to measure the hardenability of steel by spraying coolant at the bottom surface of the standard cylindrical specimen of 25mm diameter and 100mm length for 10 minutes. However, core parts of large-scale wind turbine components at a distance from the surface exhibit low cooling rates due to the mass effect. Thus, for large-scale products, research of hardness prediction for various points through analysis methods and measurement of the hardness



variation by carrying out the hardenability test is necessary. Figure 1 shows the hardenability test method for large-scale specimens.



Fig. 1 Large size hardenability test method

Table.I shows the chemical composition of 42CrMo4 used for the large scale Jominy test.

**I.TABLE
CHEMICAL COMPOSITIONS OF TEST MATERIALS**

C	Si	Mn	P	S	Cu
0.40	0.26	0.85	0.011	0.004	0.05
Ni	Cr	Mo	Al	V	Fe
0.09	1.10	0.24	0.028	0.06	Val.

Three specimens were prepared from the external surface, 1/2R, and center of the specimen to analyze the hardness for various points of the material, in the end, quenched large scale specimen. Figure 2 shows the location points from which specimens were extracted. The extracted quadrilateral specimen blocks had dimensions of 30x30x400mm. The hardness and microstructure were measured for the quenched condition and after tempering heat treatment at 600°C and 660°C. The positions at which specimens were extracted were designated as C for the center part, S for the surface part, and R for the 1/2 point between the center and surface parts. The state of completed cooling was marked as “1,” and the specimens that underwent tempering for 1 hour at 600°C and 660°C were marked as “2” and “3”, respectively.

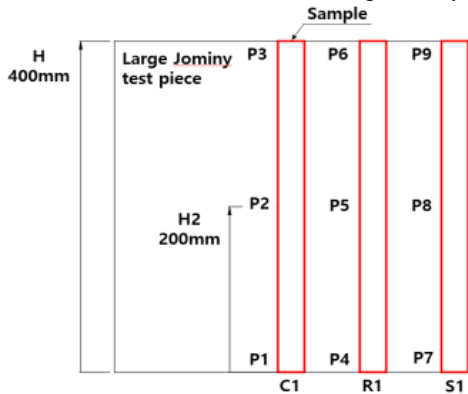


Fig. 2 Marking designations of the investigation points of the cooling specimens

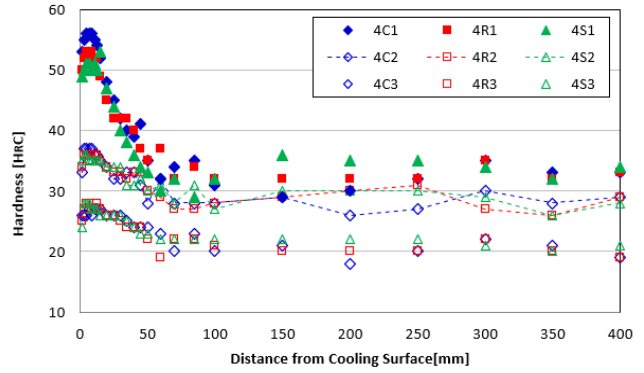


Fig. 3 Hardness variation for each position of the the42CrMo4 cooling specimen according to quenching and tempering

The hardness was measured at locations 1.5mm~400mm from the water-cooled point of the extracted cooling specimen, and the measured hardness is shown in Fig. 3.

In addition to the hardness, the microstructure and austenitic phase ASTM grain size were measured for each point for the large-scale cooling specimen. The microstructures of C1, R1, and S1 where water cooling is directly applied were martensite. Moving closer to the core part, the martensite amount decreased, and the bainite and pearlite structures increased. The ASTM grain size measurements for each point of the heat-treated “2” and “3” specimens resulted in grain sizes of 6.9 ~ 7.2.

In order to compare the temperature varies according to time at the locations of specimen extraction of the cooling specimen, Deform 3D was used to analyze the temperature varies according to the forced cooling. A 1/4 model was used, and the cooling conditions for the analysis included air cooling at the upper surface and water cooling at the lower areas. For the heat extraction coefficient of air and water, the heat transfer coefficient for the cooling of large-scale forged parts calculated from previous studies was used.[11]

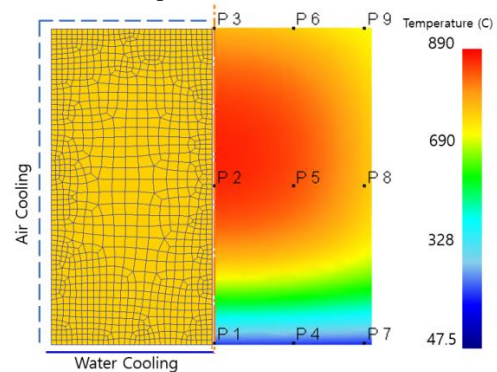


Fig. 4 Boundary conditions of FE Analysis and location of temperature investigation

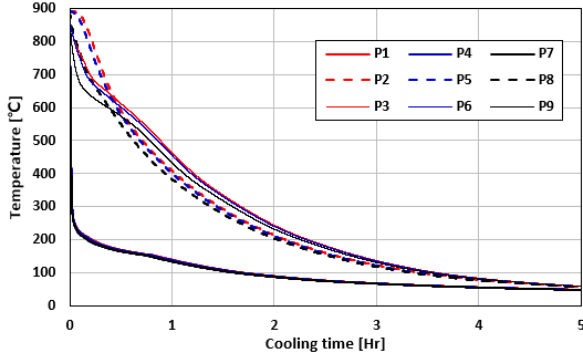


Fig. 5 Temperature history of cooling specimens

The boundary conditions of the heat transfer analysis and the temperature analysis results of the 9 points P1 ~ P9 shown in Fig. 3 are shown in Fig. 4 and Fig. 5. In Fig. 4, the heat extraction coefficient of water is applied to the area in contact with water, and the coefficient of air is applied to the sides and upper area. So, P1, P4, and P7 in the lower area are cooled rapidly while P2 and P5 in the core part and P3, P6, P8, and P9, which are external points in contact with the air at the start of the cooling, are cooled relatively slowly. However, after 25 minutes from the start of the testing, the temperature of the core part was observed to decrease further due to the water cooling, as shown in Fig. 5.

B. Hardness Prediction from Quenching

The CCT curve of 42CrMo4 used in the test was determined using Jmatpro. The cooling curve of the measurement position can be inputted into the CCT curve to predict the volume fraction, hardness, and strength. The prediction points for the hardness after quenching were P1 ~ P9 shown in Fig. 2, and Deform3D was used to calculate the cooling curve for each point with respect to time. The quench property module of Jmatpro was used to calculate the hardness, mechanical properties, and composition fraction. Figure 6 shows the CCT curve overlapped with the cooling curves of P1 ~ P9.

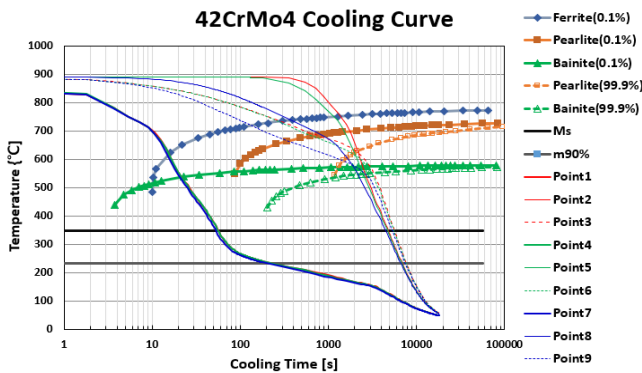


Fig. 6 The CCT curve of 42CrMo4 and the temperature v ariation for each point of the cooling specimen

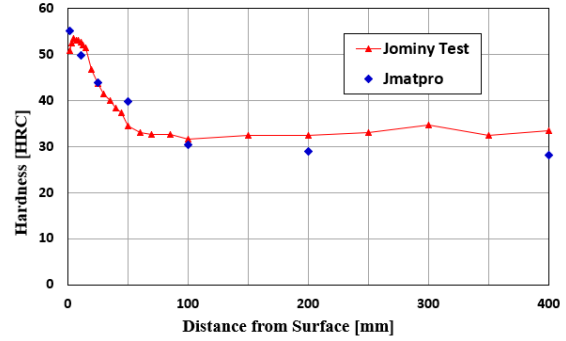


Fig. 7 Comparison of hardness measurement and Jmatpro prediction results of Jominy specimen

The hardness calculation of Jmatpro was carried out for the points 1.5, 11, 25, 50, 100, 200, and 400mm from the quench end surface. A comparison of the calculation and measurement results is shown in Fig. 7. In the hardness calculation of Jmatpro, differences in hardness were observed according to the austenite grain size, and Fig. 7 shows the calculation result with the input of 7.0.

C. Hardness Prediction Model Considering Tempering

The prediction of strength and structure using the phase fraction according to the phase transforming due to quenching can be calculated using the CCT curve and cooling rate of the material. However, tempering after quenching induces strength and hardness degradation. The effect of tempering is influenced by the heat treatment temperature and time, so the tempering parameter can be expressed as Eq. (1).

$$M = \frac{T}{1000} (20 + \log(t)) \tag{1}$$

The value of M for the tempering parameter presented above for tempering at temperatures of 873K(600°C) and 933K(660°C) for 1 hour each was calculated to be 17.46 and 18.66, respectively. A linear equation for the hardness after quenching and hardness variation after tempering was possible, and an equation was to be derived.

In order to reduce scattering for each point, the averages of the hardness variation were taken for each cooling point of the 42CrMo4 center part, 1/2R, and surface part, and a regression equation can be derived for the hardness distribution for each point with regard to tempering at 600°C and 660°C.

$$HRC = \frac{a}{(1 + be^{-\alpha})} \tag{2}$$

The parameters of hardness equation (2) are calculated respectively according to the tempering parameters for 17.46 and 18.66 and shown in Table 2. Figure 8 shows the hardness curve obtained through the regression equation and the experiment results together.

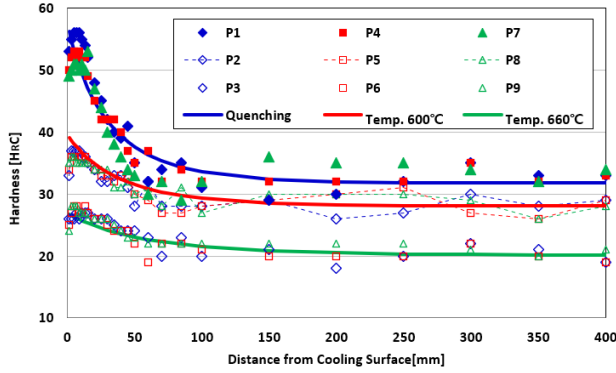


Fig. 8 Comparison of the hardness distribution of the measurements and regression equation

II. TABLE
VARIABLE OF THE REGRESSION EQUATION

Material	Tempering Parameter	a	b	c
42CrMo4	Quenching	31.7655	- 0.4492	0.0212
	17.46	28.0702	- 0.2900	0.0195
	18.66	20.1705	- 0.2500	0.0137

III. Quantitative Model Verification

A. Strength and Hardness Measurement by Location for Large Scale Parts

The hardness and tensile strength of a wind turbine main shaft of 42CrMo4 that underwent quenching at 900°C followed by tempering at 640°C for the various points were measured. Hardness variation of the surface and core part due to the mass effect was predicted, so specimens were extracted at locations 12.5, 75, 150, and 225mm from the surface and all 150mm from the shaft end. Table 3 shows the tensile test and hardness measurement results for the specimens, and Fig. 10 shows the strength and hardness variation graph.

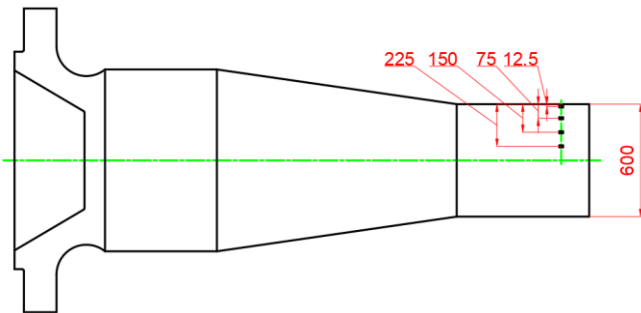


Fig. 9 Main shaft specimen extraction locations

III. TABLE
MAIN SHAFT FRACTURE TEST RESULT

Depth [mm]	Test	YS [MPa]	TS [MPa]	EL [%]	Hardness [HRC]	ASTM No.
12.5	1st	717	871	22	26.4	7.41
	2nd	717	869	23	27.2	7.23
	3rd	720	873	22	27.1	7.32
	Ave.	718	871	22.3	26.9	7.32
75	1st	642	824	21	26.0	7.14
	2nd	648	828	22	26.3	7.36
	3rd	645	825	22	25.6	7.28
	Ave.	645	825.7	21.7	26	7.24
150	1st	605	784	21	24.1	6.95
	2nd	607	783	22	23.7	6.79
	3rd	609	783	21	24.0	7.04
	Ave.	607	783.3	21.3	23.9	6.93
225	1st	594	773	21	22.7	7.00
	2nd	595	772	21	21.3	6.74
	3rd	597	774	21	23.0	7.18
	Ave.	595.3	773	21	22.3	6.97

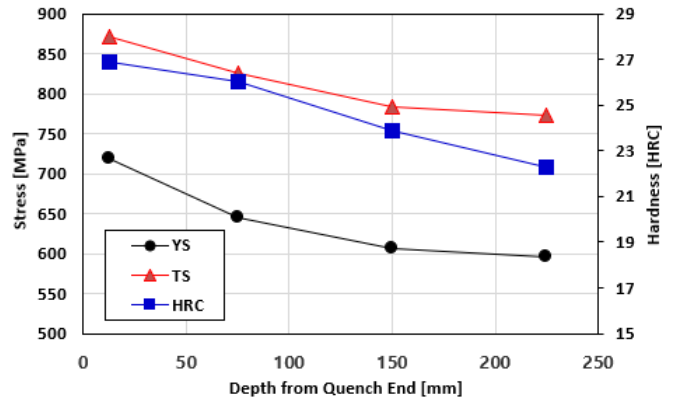


Fig. 10 Tensile strength and hardness distribution for the location points of the fracture specimens

B. Hardness Prediction using Jmatpro

The main shaft is a large-scale production with a shaft diameter of $\Phi 675\text{mm}$ and length of 4,500mm, so a maintenance time of 30 minutes for every maximum thickness of 25mm is set for the material uniformity for heat treatment. After heating to the target temperature, a set temperature is maintained within a furnace, followed by quenching. The quenching heat treatment was analyzed so that convective heat transfer occurred on all surfaces in contact with the coolant by applying the axial symmetry condition using Deform 2D. The boundary conditions are shown in Fig. 11. As shown in Fig. 12, the temperature was tracked at locations 12.5, 75, 150, and 225mm from the surface and all 150mm from the end of the main shaft.

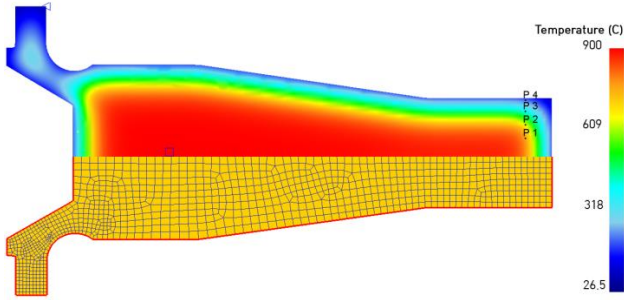


Fig. 11 The boundary conditions of cooling analysis and the temperature distribution for various points

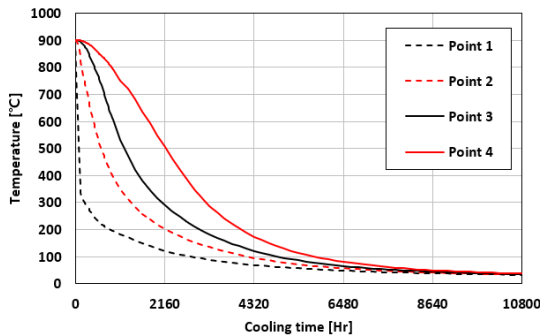


Fig. 12 Temperature gradient through the cooling analysis

The hardness was calculated using the temperature gradient for the various points in Fig. 12 and the quenching property module of Jmatpro. The input quenching property values were the alloy composition and ASTM grain size before quenching shown in Table 1. In this analysis, the grain size number 6.74 of the core part analyzed in the fracture specimen from Table 4 was inputted. The hardness calculation result due to the quenching process is shown in Table 5.

IV. TABLE

HARDNESS CALCULATION OF QUENCHED SHAFT

Depth from surface	12.5mm	75mm	150mm	225mm
Hardness[HrC]	42.6	33.92	32.24	31.27

C. Hardness Calculation After Tempering

After measuring the hardness distribution from the surface in the large-scale cooling test and carrying out tempering for 1 hour at 600°C and 660°C, the hardness variation according to the tempering heat treatment was quantified as Eq. (2) and Fig. 8. The final main shaft product was heat-treated at 640°C. The tempering parameter is affected by temperature as well as time. However, in this study, the tempering maintenance time was set to 30 minutes of tempering heat treatment time per inch as recommended by ASTM specifications, so the time was calculated as “1” in the tempering parameter calculation. For verification of the possibility of hardness variation prediction due to tempering, the hardness for the various points of the large-scale Jominy test was predicted using Deform and Jmatpro and compared

with the experiment result in Fig. 7. The regression equation for the tempering conditions of 873K(600°C) and 933K(660°C) is shown in Eq. (2) and Table 2 to quantify the hardness degradation due to tempering according to the tempering condition. The tempering heat treatment temperature of the fractured main shaft is 640°C. Thus, the tempering parameter calculated for a constant heat treatment time of 1 hour according to specifications results in 18.26. Interpolation of the tempering parameter and hardness equation variables from the values of Table 2 results in the hardness plot as shown in Fig. 13.

Plotting the positional hardness in Fig. 13 calculated using Jmatpro as shown in Table 4 in the previous section results in calculations marked the red square points in the figure. Here, the hardness of the 12.5mm point is lower than that of the large-scale cooling specimen, so it is moved to the 25mm point where the hardness becomes 42.6HRC to match the hardness. A comparison of the hardness for the tempering temperature of 640°C and the hardness for the various points of the fracture specimen at the moved position shows similar hardness distributions as marked by the triangle points in Fig. 13.

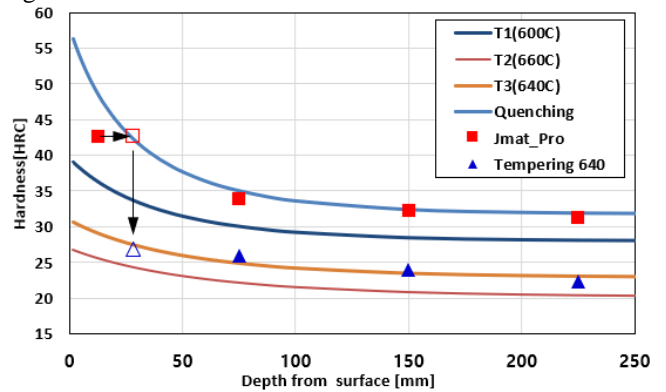


Fig. 13 Calculation method of the hardness distribution after tempering considering the tempering conditions and hardness value

Expressing the hardness prediction above in Table 5 and Fig. 14 revealed that the prediction result error does not exceed 4.8%.

V. TABLE

COMPARISON BETWEEN EXPERIMENT AND HARDNESS PREDICTION RESULTS

Depth	Test Hardness	Hardness by eq.	Deviation	Ratio
12.5	26.9	28.2	-1.3	-4.8%
75	26	24.8	1.2	4.6%
150	23.9	23.4	0.5	2.1%
225	22.3	23	-0.7	-3.1%

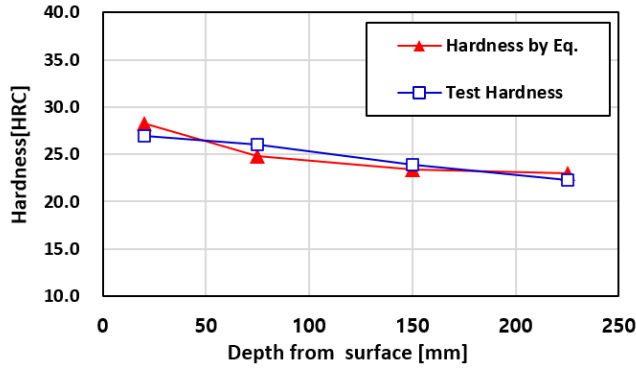


Fig. 14 Comparison between the experiment and predicted hardness distribution for the various points

IV. CONCLUSIONS

In order to predict the hardness and strength of material considering the mass effect of a large scale forged part, hardenability testing of the large scale specimen, hardness measurement and regression analysis according to the heat treatment, Deform and Jmatpro analyses, and quantification of the hardness softening due to tempering are carried out, and the following conclusions were obtained.

1) After end quench cooling of a 400x400x400mm large scale cooling specimen and extraction of specimens, the positional hardness distributions for the quenched state and tempering temperatures of 600°C and 660°C were measured to express the positional hardness according to the heat treatment condition as a regression equation.

2) Comparison between the positional hardness from the end quench surface of the large scale cooling specimen and the prediction result obtained using Deform 2D, and Jmatpro revealed similar hardness distributions. The hardness from the analysis showed differences between the cooling temperature gradient and austenite grain size.

3) In order to investigate the hardness prediction capability using finite element analysis and the hardness softening regression equation, fracture analysis was conducted for the main shaft that underwent quenching at 900°C and tempering at 640°C. Calculation of the hardness prediction results from the quenching analysis using the tempering softening curve showed that the hardness can be predicted with errors of 4.8% or lower.

ACKNOWLEDGMENT

This work was supported by the Korea Institute of Energy Technology Evaluation and Planning (KETEP) and the Ministry of Trade, Industry & Energy (MOTIE) of the Republic of Korea (No. 202000580002).

REFERENCES

- [1] Y.C. Kwon, J.H. Kang, and S.S. Kim, Study on Manufacturing Process of Hollow Main Shaft by Open Die Forging, Trans. Korean Soc. Mech. Eng. A, 40(2) (2016) 221-227.
- [2] T. Wei, Wind power generation and wind turbine design, WIT press, Billerica, USA,(2010).
- [3] S. Mitsuru, T.Ikuo, S. Junichi and S. Takashi, Development of 5-MW Offshore Wind Turbine and 2-MW Floating Offshore Wind Turbine Technology, Hitach Review, 63 (2014) 414-421.
- [4] ISO 683-11, Heat-treatable steels, alloy steels, and free-cutting steels — Part 11: Wrought case-hardening steels, (1987).
- [5] EN10083, Steels for quenching and tempering - Part 3: Technical delivery conditions for alloy steels ,(2007).
- [6] JIS G4052, Structural steels with specified hardenability bands, (2008).
- [7] J.H. Kang and H.W. Lee, Structural Safety Analysis of Main Shaft for Wind Power Generators Considering Mass Effect, International Journal of Applied Engineering Research, 12 (2017) 6862-6869.
- [8] A. R. George, R. M. Samson, K. Ottoor, T. Geethapriyan, The Effects of Heat Treatment on The Microstructure and Mechanical Properties of EN19 Steel Alloy, IJMSE, 6(2) (2018) 56-66
- [9] A.Sugianto, M.Narazaki, M.Kogawara and A.Shirayori, A comparative study on determination method of heat transfer coefficient using inverse heat transfer and iterative modification, Journal of Materials Processing Technology, 209 (2009) 4627-4632.
- [10] H.S. Hasan, M.J. Peet, J.M. Jalil, and K.D.H.Bhadeshia, Heat Transfer Coefficients during Quenching of Steels, Heat and Mass Transfer, 47 (2011) 315-321.
- [11] A.Buczek and T.Telejko, Investigation of heat transfer coefficient during quenching in various cooling agents, International Journal of Heat and Fluid Flow, 44 (2013) 358-364.
- [12] J.H. Kang and Y.C. Kwon, Study on prediction of mechanical properties of the large ring-shaped forging depending on cooling rate, International Journal of Mechanical Engineering and Technology, 10 (2019), 109-119.
- [13] J. Hu., L.X. Du, H.Xie, X.H. Gao, and R.D.K.Misra, Microstructure and mechanical properties of TMCP heavy plate microalloyed steel, Materials Science & Engineering A, 607 (2014) 122-131.
- [14] X.W. and L.Y. Lan, Optimization of mechanical properties of low carbon bainitic steel using TMCP and accelerated cooling, Procedia Engineering, 81 (2014) 114-119.
- [15] T. Mohankumar, K. Rajan, P. Naveenchandran, K Sivakumar, Heat Transfer Characteristics of Double Pipe Heat Exchanger with Plain Twisted Tape Insert Using Titanium Oxide, IJITEE, 8(11) (2019) 3909-3911
- [16] B.O. Kim and O.Y. Lee, The Study of Nuclear Reactor Pressure Vessel Steel SA508Gr.3 Mechanical Properties and Temper-Parameter, J. of the Korean Society for Heat Treatment, 25(3) (2012) 121-125.
- [17] F.S. Vicente, J.C. Carrasco, R.F. Antoni, J.C.F.Taberner and M.P.Guillamón, Hardness Prediction in Quenched and Tempered Nodular Cast Iron Using the Hollomon-Jaffe Parameter, Metals, 11(2) (2021) 297.